

AN EFFECT OF BALL MILLING ON MICROSTRUCTURAL PARAMETERS OF NANOSTRUCTURED MoO_3 - CuO - V_2O_5 COMPOSITE NANOPOWDERS

T. VIJAYA KUMAR¹ & K. V. RAMANA²

¹Research Scholar, Department of Mechanical, Koneru Lakshmaiah Education Foundation,
Vaddeswaram, Andhra Pradesh, India

²Professor, Department of Mechanical, Koneru Lakshmaiah Education Foundation,
Vaddeswaram, Andhra Pradesh, India

ABSTRACT

The present work meant to look at the impact of crystalline size, lattice strain and dislocation density of ultrafine thermally exfoliated MoO_3 , MoO_3 - CuO and MoO_3 - V_2O_5 composite nanopowders utilizing mechanochemical milling process at various time intervals. The characterization of the nanocomposite synthesized powders was characterized by a range of spectroscopic features such as Powder X-Ray diffraction, Scanning Electron Microscope and Electron Dispersive X - Ray Spectroscopy. With the X - Ray peak profile demonstration, the orthorhombic phase of MoO_3 , V_2O_5 and monoclinic phase of CuO were shown. On the basis of XRD, Debye - Scherrer and W - H calculations the average crystalline size, lattice strain and dislocation density evaluated were almost equal. SEM images of MoO_3 , MoO_3 - CuO confirm that the irregular shaped particle sizes and MoO_3 - V_2O_5 displays the spherical structures irregularly shaped and deposited with vanadium flakes. The presence of constituent elements of prepared samples is confirmed by EDS spectrum.

KEYWORDS: Nanopowders, Ball Milling, XRD, W-H Plot, Lattice Strain & SEM Images

Received: Feb 15, 2019; **Accepted:** Mar 09, 2019; **Published:** Apr 13, 2019; **Paper Id.:** IJMPERDJUN201914

1. INTRODUCTION

Due to their interesting applications as catalysts, sensors and photo chromatic devices, transition - metal oxides emerged as a new type of research materials [1-4]. Among these materials, Molybdenum trioxide (MoO_3) is attractive as its structural and optical properties, and is a broad band gap ($> 2.7\text{eV}$) type n- semiconductor. Nanotechnology also offers a large field of tribological research. Molybdenum oxides, of course, are divided into orthorhombic α - MoO_3 stable thermodynamically and β - MoO_3 monoclinic metastable phases. Molybdenum (IV) oxide exists in three distinctive phase structures as thermodynamically stable orthorhombic (α - MoO_3), monoclinic (β - MoO_3) and hexagonal (h- MoO_3). It has a tremendous zone of utilizations, for example, photo chromatic materials which changes drab to blue by ultraviolet illumination, conductive gas sensors, smart windows, lubricants and catalysts. MoO_3 is utilized as a solid lubricant as it offers coefficient of friction of almost 0.2 at high temperature of about 700°C . The friction and wear conduct of MoO_3 were dissected at high temperatures with Aluminum bronze and considerable outcomes were inferred. Nanocomposites of MoO_3 based, for ex. MoO_3 - CuO MoO_3 - NiO and MoO_3 - ZnO are considered for their predominant tribological properties at raised temperatures[5].

Cupric Oxide (CuO) is an indirect band gap of 1.1-1.6eV p-type semiconductor. CuO nanoparticles can likewise be utilized as strong lubricants because of their obvious friction reduction properties. Most lamellar /

layered solid lubricants fail in open air for lubrication applications, and the temperature exceeds 500 °C when they become oxides. Important research was conducted for the use of transition metal oxides as lubricants and for the formation of alloys or composites for higher temperatures of highly capable lubricants[6-8]. These oxides can form into mixed oxides for wider operational ranges that is composites or alloys for significant uses with monoxide lubricants. Blended oxide, for ex. MoO_3 - CuO can give upgraded frictional execution at various high temperatures.

For its many applications, such as optical, electrical, memory and cathode materials for building solid - state devices V_2O_5 has become an important element for technology. Because of the accessibility of multiple oxidation states, Vanadium - based catalysts are known to be effective for oxidation chemistry, and therefore Vanado - silicates are potentially interesting catalysts[9 - 11].

The present work aimed at comparing the effect of MoO_3 , $\text{MoO}_3\text{-CuO}$ and $\text{MoO}_3\text{-V}_2\text{O}_5$ composite nanopowders using planetary ball milling method at different time periods using crystalline size, lattice strain and dislocation density. The synthesized composite nanopowders were characterised with spectroscopic characteristics such as X - Ray diffraction (PXRD) and Scanning Electron Microscope (SEM) with EDX.

2. MATERIALS AND METHODS

2.1 Materials

The following conventional powders includes MoO_3 , V_2O_5 , and CuO procured from Merck chemicals (India). The chemical reagents have an analytical grade and are used without further cleansing. In the synthesis, the chemical products used are of more than 99.5% pure.

2.2 Synthesis Procedure

Different nanocomposite syntheses are planetary ball milling, vapor deposition, plasma arcing, sol – gel method etc. Present work has been performed using the ball milling method in five samples at different periods[12] for preparing orthorhombic MoO_3 , $\text{MoO}_3\text{-CuO}$ and $\text{MoO}_3\text{-V}_2\text{O}_5$ composite nano powders. MoO_3 , CuO , and V_2O_5 powders of mean size $5\mu\text{m}$ were considered (weight proportions of MoO_3 and CuO as 2.3:1 & 3.3:1 and for $\text{MoO}_3\text{-V}_2\text{O}_5$ as 1:1 were homogeneously mixed separately). Ball milling was performed by taking powder to ball ratio in the range of 1:5 to 1:10. For 2, 4, 6, 8, 10 and 20 hours, the milling took place at 5 minutes interval after every 30 minutes with rotation speeds of 350 rpm respectively. The ball mill consists of Zirconium balls as medium in milling. The mixtures obtained were taken in a crucible and calcined at 200 ° C in air for 3 hours.

2.3 Characterisation

MoO_3 , $\text{MoO}_3\text{—CuO}$ and $\text{MoO}_3\text{-V}_2\text{O}_5$ Nanocomposite Powder of X Ray diffraction (XRD) was performed on a Cu - $\text{K}\alpha$ radiative XPert Pro - diffractometer ($\lambda=1.5406 \text{ \AA}$). The readings were taken at a range of 10°-80° on 2θ with a step size of 0.05° in 40KeV at 15mV applied current. The phase distribution, SEM images were obtained from a Carl Zeiss SEM EVO with carbon coating and presence of constituent elements of prepared samples are confirmed from ZEISS EVO 18.

3. RESULTS AND DISCUSSIONS

3.1 PXRD Analysis for Molybdenum Trioxide (MoO₃)

The X-Ray diffraction pattern [13-14] was used to perform the crystal structural phase of the synthesized MoO₃ nanopowders. The diffraction peaks shown (Figure 1) by the synthesized powders emphasize the phase structure as a system of orthorhombic crystal (α -MoO₃), which has appropriate cell parameters, $a=3.952$ and $b=13.868$ and $c=3.687$ nm. The diffraction peaks of the nanopowders are matched with JCPDS file no. 05 - 0508 diffraction data, no difference in phase structure is observed with respect to the milling time.

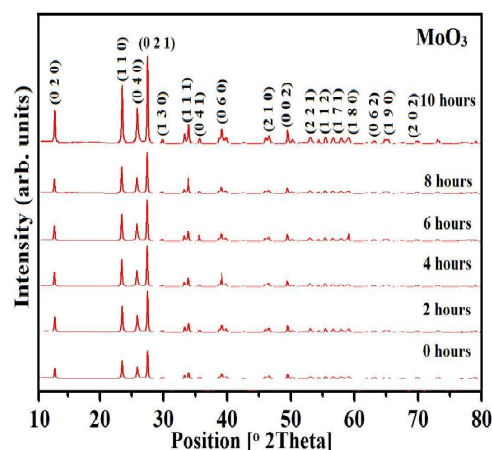


Figure 1: XRD Peaks of Ball Milled MoO₃ Nanopowders

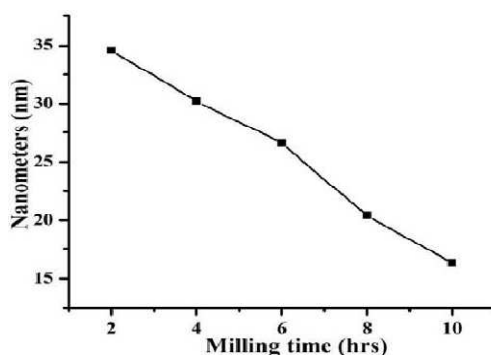


Figure 2: Milling Time Vs Crystal Size of MoO₃ Nanopowders at Different Intervals

The existence of sharp diffraction peaks reveals as shown in Figure 1, the formation of pure MoO₃ Nanopowders. Simple and powerful X - ray peak analysis is used to estimate the crystalline size and micro strain.

3.1.1 Crystal Size

The average crystalline size of the samples produced is calculated using the formula of the Debye - Scherrer as shown in the equation (1).

$$D_s = (0.9 \lambda) / (\psi \cos \theta) \text{ nm} \quad (1)$$

Where D_s is the crystallite size, λ is the wavelength of X-ray ($\lambda = 0.155$ nm for Cu-K α), ψ is the Full Width at Half Maximum (FWHM) of the Bragg's peak (in radians), θ is the diffraction angle of the reflection[15].

The average crystalline size ' D_s ' is calculated from the diffraction peaks is found to be 35-15nm as shown in Figure 2. There is no evidence of any remaining impurities or bulk materials [16].

3.1.2 Micro Strain

Lattice strain is a measure of lattice constants distribution resulting from crystal imperfection such as dislocation of the lattice using the equation (2). From Stokes Wilson Formula [17], the micro strains induced expansion in powders due to crystal imperfection and distortion were calculated. It is observed that micro strain increases with the increase in milling time. Table1 summarizes the values of lattices train of MoO_3 Nanopowders synthesized at various milling intervals.

$$\varepsilon = (\psi \cos \theta) / 4 \quad (2)$$

Figure 2 shows that MoO_3 average crystalline size gradually decreases as the ball milling time increases. At 10 hours of ball milling, the least size was found producing 16.5 nm sized crystals. The average crystal sizes are shown in Table1 at different time intervals.

3.1.3 Dislocation Density

The twist of the high speed ball and vial is in the crystal, resulting in the ball milling dislocations of the same way as a screw. Coriolis and centrifugal forces[18] accelerate the grinding balls. Dislocation density (δ) was estimated by equation(3).

$$\delta = 1 / (D_s)^2 \quad (3)$$

Where ' D_s ' is the crystalline size.

With increasing ball milling time, the dislocation densities of the samples increase. The dislocation density values for different time intervals are shown in Table 1.

Table 1: Comparison of MoO_3 Nanopowder Average Crystalline Size, Lattice Strain, and Dislocation Density Synthesized at Various Milling Times

Milling Time (hours)	Crystalline Size (Scherrer's Equation)	Micro-Strain ($\varepsilon \times 10^{-3}$)	Dislocation Density ($\delta \times 10^{15} \text{ m}^{-2}$)
2	34.6	0.02	0.835
4	30.2	0.27	1.096
6	26.6	0.31	1.413
8	20.4	0.35	2.402
10	16.3	0.37	3.763

3.2 PXRD for Molybdenum Trioxide and Vanadium Pentoxide($\text{MoO}_3\text{-V}_2\text{O}_5$)

As shown in Figure 3 [18], XRD composite nanopowder of $\text{MoO}_3\text{-V}_2\text{O}_5$ have been executed on a PAN alytical Xpert pro-diffractometer with $\text{Cu-K}\alpha$ radiation ($\lambda=1.55^\circ\text{A}$). The measurements were made at a range of $10^\circ - 80^\circ$ on 2θ with a step size of 0.05° . X-Ray Diffraction pattern exhibit orthorhombic crystal system ($\alpha\text{-MoO}_3$) and ($\alpha\text{-V}_2\text{O}_5$) with corresponding lattice parameters $a=3.965$, $b=13.87$ and $c=3.70\text{nm}$ and that of V_2O_5 as $a=11.55$, $b=3.55$ and $c=4.40 \text{ nm}$ diffraction peaks of the composite are well matched with standard diffraction data of JCPDS file numbers 05-0509 and 77-2417.

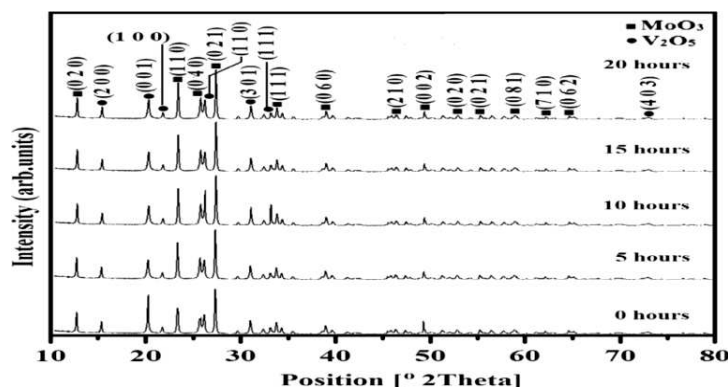


Figure 3: PXRD Patterns of MoO₃-V₂O₅ Ball Milled Composite Nanopowders

3.2.1 Crystal Size

The estimation of crystalline size and lattice strain is done by simple and powerful X-Ray profile analysis. The average crystalline size of the prepared samples were calculated using the Debye-Scherrer's formula given in the equation(4).

$$D_s = (0.9 \lambda) / (\psi \cos \theta) \text{ nm} \quad (4)$$

The average crystalline size ' D_s ' is calculated from the diffraction peaks ranges from 86-10nm on the variation of milling time as tabulated in Table2. It is clearly shown from Figure 4 that the average crystalline size decreases with increasing milling time and was 10 nm with 20 hours of milling time. No structural changes are observed with regard to the milling time.

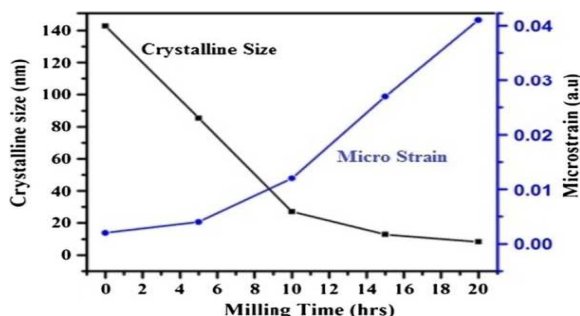


Figure 4: Crystallite Size and Lattice Strain at Various Milling Intervals

3.2.2 Micro Strain

Ball milling synthesis induces a considerable strain on the composite nanopowder manufactured. Micro strain is a measure of distribution of lattice constants. Crystal imperfections such as lattice dislocations have an effect on the formation of these lattice constants. The Stokes – Wilson equation(5) was used to detect the micro strain (ϵ) that induced powder expansion because of crystal imperfections and distortions. The variation of lattice strain with milling time is as shown in Table 2, resulting in increased lattice strain over milling time. Figure 5 shows that the strain of the lattice increases gradually as the milling time increases.

$$\epsilon = \frac{\psi \cos \theta}{4} \quad (5)$$

A comparative evaluation of $\text{MoO}_3\text{-V}_2\text{O}_5$ composite nanopowders obtained from X - Ray diffraction (XRD) data and W-H plot is reported for the average crystal size and lattice strain. Assuming that particle size and line expansion contributions are independent from each other.

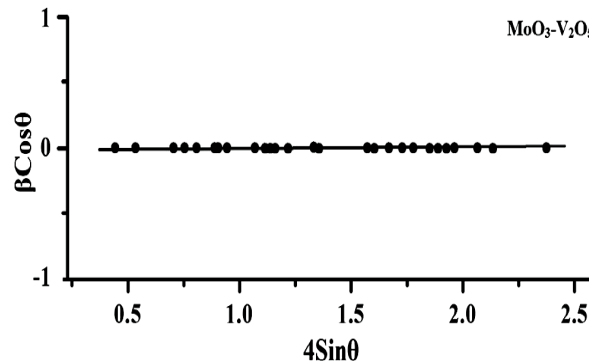


Figure 5: Williamson-Hall Plot of $\text{MoO}_3\text{-V}_2\text{O}_5$ Nanocomposite Powders

3.2.3 Dislocation Density

The high speed ball and vial rotations produce a twist in the crystal resulting in a screw like ball milling dislocations. Through coriolis and centrifugal forces the grinding balls are accelerated. The dislocation density (δ) was calculated by the equation (6).

$$\delta = \frac{1}{D_s^2} \quad (6)$$

3.2.4 Williamson-Hall Analysis

W-H analysis is a simplified integral breadth method employed for estimating crystal, crystallite size and micro strain, considering the peak width as a function of 2θ .

$$\psi \cos \theta = \frac{0.9\lambda}{D_s} + 4\epsilon \sin \theta \quad (7)$$

Equation (7) represents W-H plot, assumes the strain is uniform in each crystallographic directions. It represents a straight line between $4S \sin \theta$ (on X-axis) and $\psi \cos \theta$ (on Y-axis). The crystalline size (D_s) and lattice strain (ϵ) are calculated from the intercept ($k\lambda/D_s$) and slope of the line. The milling time effect on dislocation densities is as shown in Table 2. Consequently, there is a gradual increase in dislocation densities as shown in Table 2 on the increase in milling time.

Table 2: Average Crystallite Size, Lattice Strain and Dislocation Density of $\text{MoO}_3\text{-V}_2\text{O}_5$ Composite Nanopowders Synthesised at Various Time Intervals

Milling Time (Hours)	Crystalline Size (Scherrer's)	Micro Strain ($\epsilon \times 10^{-3}$)	Dislocation Density
0	142.7	0.002	0.049
5	85.38	0.004	0.137
10	26.97	0.012	1.37
15	12.81	0.027	6.09
20	8.30	0.041	14.49

3.3 Molybdenum Trioxide and Copper Oxide ($\text{MoO}_3\text{-CuO}$)

The diffraction peaks of the Nanocomposite powders show two different phase structures coexisting with

corresponding lattice cell parameters, such as orthorhombic crystal structure system (α -MoO₃) with $a=3.97$, $b=13.86$ $c=3.70$ nm and CuO exhibits monoclinic system with lattice parameters as $a=4.69$, $b=3.43$, $c=5.14$ nm. Figure 6 shows all composite diffraction peaks well matched with the standard diffraction data for MoO₃-CuO of JCPDS file no. 05 - 0508 & 80 – 1916.

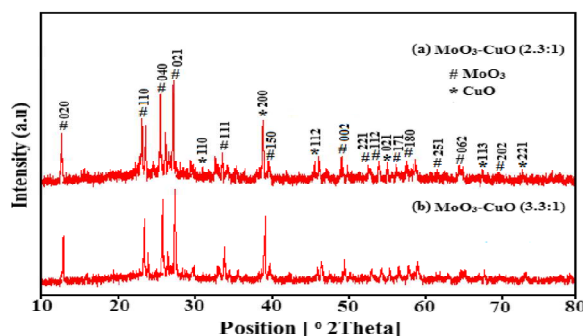


Figure 6: XRD Patterns of a 2.3:1 and b 3.3:1 MoO₃-CuO Metal Oxide Ball Milled Composite Nanopowders

3.3.1 Crystal Size

The average crystalline sizes of the prepared samples were calculated using the Debye-Scherrer's formula as given in equation(8).

$$D_s = \frac{0.9 \lambda}{\psi \cos \theta} \text{ nm} \quad (8)$$

The average crystalline size D_s is calculated from the XRD peaks. It was found to be 15 and 26 nm for the sample A and the sample B respectively. It was understood that with increase in MoO₃ content the crystalline size gradually increases.

3.3.2 Micro Strain

The micro strain(ϵ) induced broadening in powders due to crystal defect and distortion was calculated using the equation(9). From Figure 7 the plot shows the increase of micro strain with respect to increase of milling time.

$$\epsilon = \frac{\psi \cos \theta}{4} \quad (9)$$

3.3.3 Dislocation Density

X-Ray line broadening was used to estimate the dislocation densities in the samples. The dislocation density (δ) was calculated by the equation(10).

$$\delta = \frac{1}{D_s^2} \quad (10)$$

3.3.4 Williamson-Hall Analysis

The size of crystallite is not the same as particle size, as the size of crystallite is assumed to be the size of acoherently diffracting domain.

$$\psi \cos \theta = \frac{0.9 \lambda}{D_s} + 4 \epsilon \sin \theta \quad (11)$$

Equation (11) is W-H equation, assumes the strain is uniform in every crystallographic directions. Figure 7 shows

the Williamson-Hall plots of A and B samples. Lattice strain of low Molybdenum sample, i. e. A is greater than the B. Compared to the calculations of W - H plots, the crystalline sizes calculated from debye–scherrer and micro strains are found to be closely matched (Table 3).

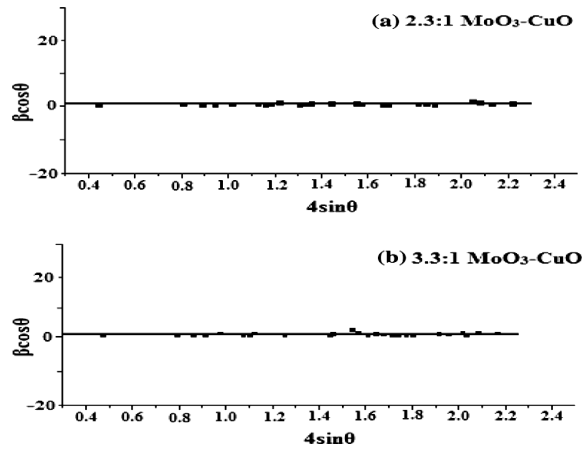


Figure 7: Williamson–Hall Plot for MoO₃-CuO Metal Oxides of 2.3:1 & 3.3:1 Composite Nanopowders

Table 3: Crystalline Size, Lattice Strain and Dislocation Density of MoO₃-CuO Mixed Composite Nanopowders of 2.3:1 & 3.3:1

MoO ₃ -CuO Sample	Crystalline Size (nm)		Microstrain ($\epsilon \times 10^{-3}$)		Dislocation Density ($\delta \times 10^{15} \text{ m}^{-2}$)
	Scherrer's	W-H Method	Calculated	W-H Method	
2.3:1	16	17	0.02	0.48	1.73
3.3:1	25	26	0.013	0.038	3.90

3.4 Morphological Studies

Sample morphology studies are observed from SEM images. SEM analysis is an important characterization technique for the sample topography study and provides information about the particle growth mechanism, shape and size.

3.4.1 Molybdenum Trioxide (MoO₃)

The samples prepared contain spherical structures with irregular shape and dimensions. No other element was found in the EDS spectrum, resulting in the purity of the synthesized sample [18].

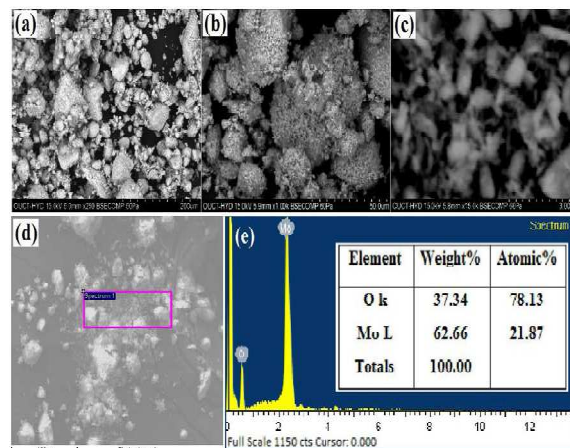


Figure 8: SEM Images and EDX Pattern of MoO₃ Ball Milled Nanopowders

3.4.2 Molybdenum Trioxide and Vanadium Pentoxide(MoO₃-V₂O₅)

Prepared samples are flake like structures. Micrographs reveals that the V₂O₅ are deposited on the surface of MoO₃ nanoclusters with irregular morphologies.

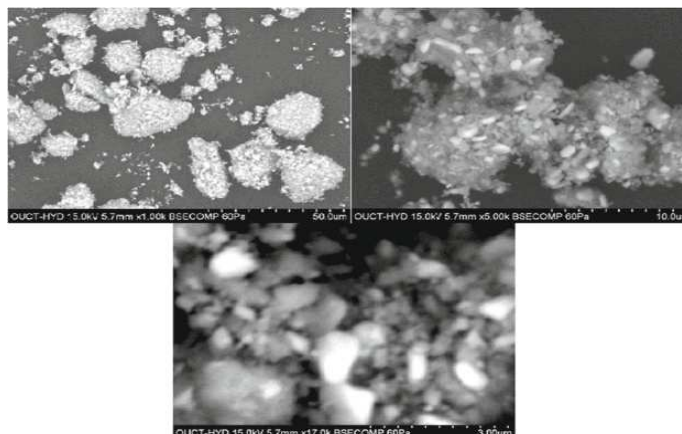


Figure 9: SEM Images of MoO₃-V₂O₅ Composite Nanopowders

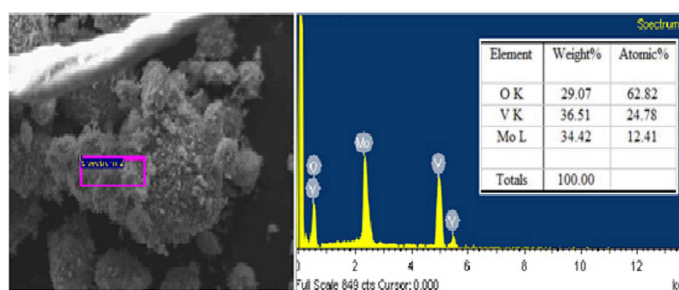


Figure 10: EDX Spectra of MoO₃-V₂O₅ Composite Nanopowders

3.4.3 Molybdenum Trioxide and Copper Oxide(MoO₃ - CuO)

The samples prepared contain rod - like and spherical structures with irregular shape and dimensions. No other element was found in EDS spectra resulting in the purity of the synthesized sample[18].

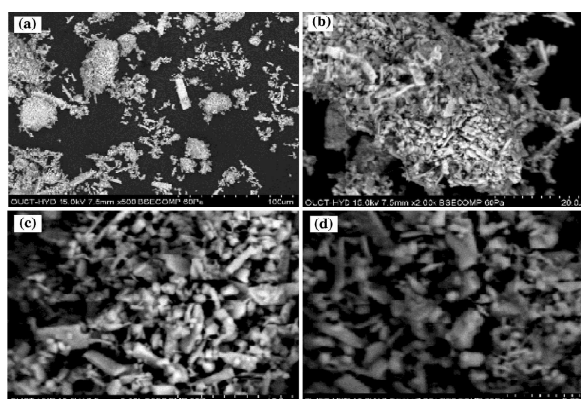


Figure 11: SEM Images of MoO₃-CuO(3.3:1) Metal Oxide Composite Nanopowders

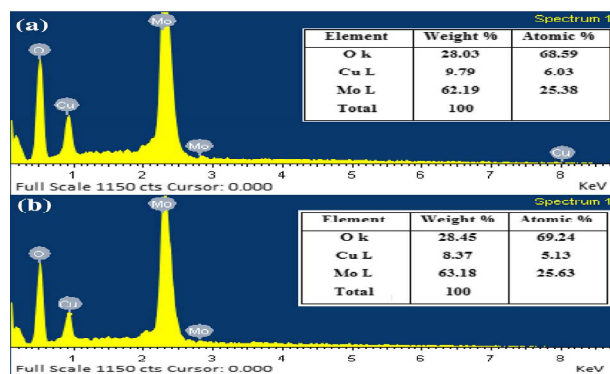


Figure 12: EDX Patterns of 2.3:1 & 3.3:1 MoO₃-CuO Metal Oxide Composite Nanopowders

4. CONCLUSIONS

The synthesis of MoO₃, MoO₃ - CuO, and MoO₃ - V₂O₅ composite nanopowders were prepared using a simple and low cost ball milling method. The orthorhombic phase structured for MoO₃, coexistence of two phase structures orthorhombic for MoO₃ and Monoclinic for CuO and orthorhombic phase structure for MoO₃ - V₂O₅, are indicated in the Powder XRD diffraction patterns for prepared composite nano powders. The crystalline dimension is calculated from diffraction data using the formula Debye - Scherrer that is counter checked by the W - H method. Results show that, with the increase of milling time lattice strain and dislocation density, the average crystalline size of composite nano powder decreases. Morphology obtained from MoO₃, MoO₃ - CuO SEM images confirms that irregular shaped particle sizes and MoO₃ - V₂O₅ exhibit irregular shaped spherical structures with deposited Vanadium flakes. EDX spectra confirms the presence of the prepared samples constituent elements.

REFERENCES

1. A. F. Lamic-Humblot, P. Barthe, G. Guzman, L. Delannoy, C. Louis, *Thin Solid Films* (2013) 96.
2. T. Vijaya Kumar, A. Gopala Krishna, R. V. S. S. N. Ravi Kumar, DolaSundee, "Investigation and Comparison of Optical and Raman Bands of Mechanically Synthesized MoO₃Nano powders", *Materials Today: Proceedings* 3, pp.54-63(2016).
3. Song, J., Li, Y., Zhu, X., Zhao, S., Hu, Y., Hu, G.; "Preparation and optical properties of hexagonal and orthorhombic molybdenum trioxide thin films, *Mater. Lett.* 95, (2013), 190-192.
4. N. A. Chernova, M. Roppolo, A. C. Dillon, M. S. Whittingham, "Layered vanadium and molybdenum oxides: Batteries and Electrochromics", *J. Mater. Chem.* 19, (2009), 2526-2552.
5. E. Comini, L. Yubao, Y. Brando, and G. Sberveglieri, "Gas sensing properties of MoO₃ nanorods to CO and CH₃OH, *Chemical Physics Letters*, Vol. 407, no.4-6, pp. 368-371,2005.
6. DolaSundee, A. Gopala Krishna, R. V. S. S. N. Ravi Kumar, T. Vijaya Kumar, " Spectral Characterisation of Mechanically Synthesized MoO₃-CuO Nano-Composite", *Int. NanoLett.*, DOI 10.1007/s40089-015-0178-z,(2016).
7. Takeichi, Y., Chujo, N. and Uemura, M., *Tribology Online*, " Effects of Molybdenum Trioxide Properties of Aluminum Bronze under High Temperature Conditions", 2009, 135-139.
8. Cullity, BD, Stock, SR; "Elements of X-ray diffraction", (2001), 3rd ed. Prentice Hall Publication, India.
9. J. F. Xu, W. Ji, Z. X. Shen, W. S. Li, S. H. Tang, X. R. Ye, D. Z. Jia and X. Q. Xin; *J. Raman Spectrosc.* 30, (1999) 413-415.

10. Belekar, R. M., Sawadh, P. S., & Mahadule, R. K. (2014). Synthesis and structural properties of Al₂O₃-ZrO₂ nano composite prepared via solution combustion synthesis. *International Journal of Research in Engineering & Technology*, 2, 145-152.
11. Battez, H., Rico, J. E. F., Arias, A. N., Rodrigues, J. L. V., Rodriguez, R. C., Fernandez, J. M. D. J. *Wear* 261, 256–263 (2006).
12. Xue, Q. J., Liu, W. M., Zhang, Z. J., "Preparation and tribological properties of tetrafluorobenzoic acid-modified TiO₂ nanoparticles as lubricant additives", *J. Wear* 213, 29–32 (1997).
13. Hernandez Battez, A., Viesca, J. L., Gonzalez, R., Balnco, D., Asedegbega, E., Osorio, A.: *Wear*. 325–328 (2010).
14. Sliney, H. E.: *Rare Earth fluorides and oxides; an exploratory study of their use as solid lubricants at temperatures to 1800 °F*. NASA TN D-5301 (1969).
15. DolaSundeeep, T. Vijaya Kumar, A. Gopala Krishna, R. V. S. S. N. Ravi Kumar, "Mechanical Milling Influence on Lattice Vibrational Behavior of MoO₃-V₂O₅ Composite Nano-powders", *Silicon Publishers*, <https://doi.org/10.1007/s12633-018-9972-3>, (2018).
16. Joyce Stella, R., Thirumala Rao, G., PushpaManjari, V., Ch. Rama Krishna, B., Babu, J.: *Alloys and Compounds*. 628, 39–45(2015).
17. Walia S, Balendhran S, Nili H, Zhuiykov S, Rosengarten G, Wang QH, BhaskaranM, Sriram S, StranoMS, Kalantar-Zadeh K (2013) *J Prog Mater Sci*, 1443–1489.
18. T. Vijaya Kumar, K. V. Ramana and R. B. Choudary, "Spectroscopic characterization of mechanically synthesized MoO₃/TiO₂ Composite Nano-powders", *International Journal of Mechanical Engineering and Technology*, Vol.8, Issue 5, pp.1051-1063 (2017).
19. Al-Waily 'Theoretical, M. (2013). *Theoretical and Numerical Analysis Vibration Study of Isotropic Hyper Composite Plate Structural*. *International Journal of Mechanical and Production Engineering Research and Development*, 3(5), 145-164.
20. R. V. S. S. N. RaviKumar, Dola Sundeeep, A. Gopala Krishna, T. Vijaya Kumar, "Spectral Investigation of Structural and Optical Properties of Mechanically Synthesized TiO₂-V₂O₅ Nano-Composite Powders", *Materials Today: Proceedings* 3, pp.31-38(2016).

